Supplementary Materials for

Resident memory T cells form during persistent antigen exposure, leading to allograft rejection

Khodor I. Abou-Daya, Roger Tieu, Daqiang Zhao, Rayan Rammal, Faruk Sacirbegovic, Amanda L. Williams, Warren D. Shlomchik, Martin H. Oberbarnscheidt, and Fadi G. Lakkis

correspondence to: mho6@pitt.edu; lakkisf@upmc.edu

This PDF file includes:

Figs. S1 to S10

Other Supplementary Materials for this manuscript includes the following:

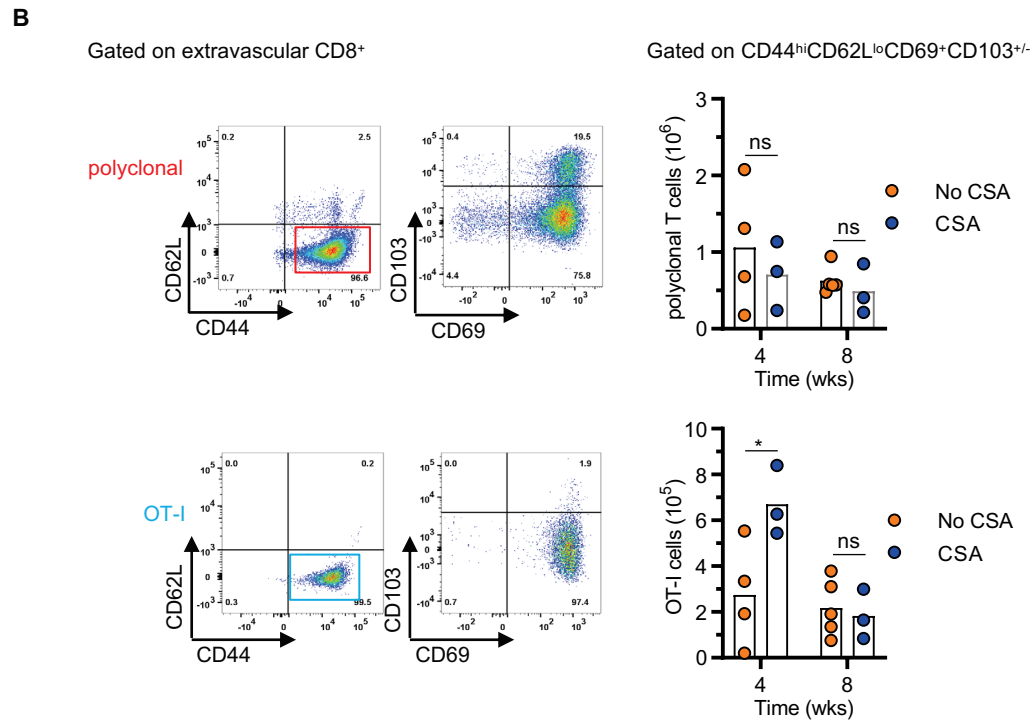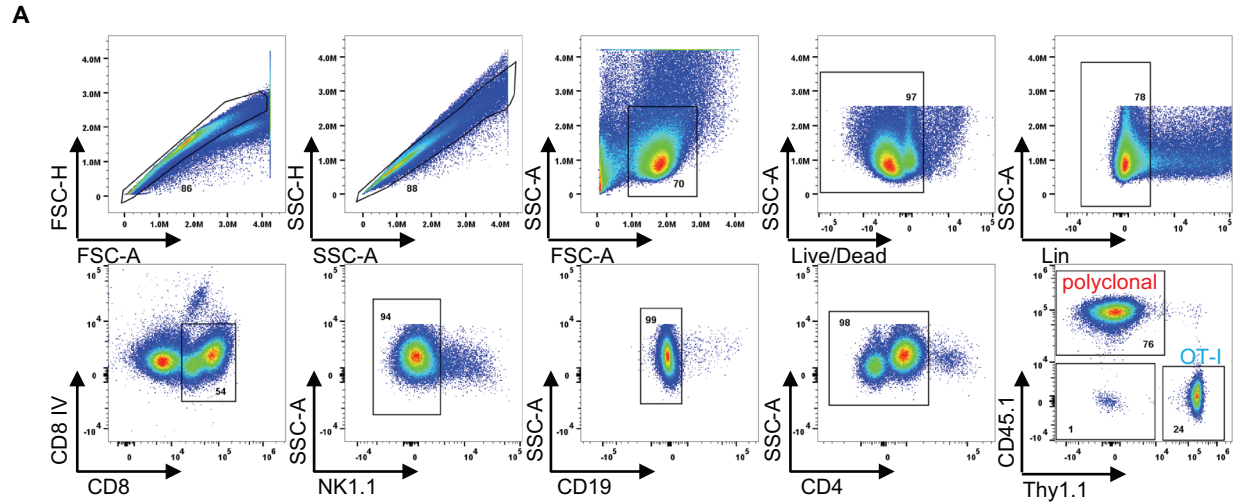|	
Canonical Pathways in OT-I T$_{RM}$	Table_S1.xlsx
Common tissue residency associated genes	Table_S2.xlsx
Canonical pathways associated with tissue residency	Table_S3.xlsx
Antibody list	Table_S4.xlsx

Figure S1. (A) Gating strategy to identify graft-infiltrating OT-I and host CD8$^+$ T cells. Lin = CD11c, CD11b, Ly6g, Ter119. **(B) Graft infiltrating CD8$^+$ T cells acquire a T$_{RM}$ phenotype in cyclosporine treated recipients.** Representative flow panels depicting the gating strategy to identify and phenotype extravascular, host polyclonal and OT-I CD8$^+$ T cells in grafts of F1.OVA + OT-I mice treated with cyclosporine for two weeks. Absolute number of graft polyclonal and OT-I CD8$^+$ T cells that acquired a T$_{RM}$ phenotype is shown in the bar graphs. Data shown are individual biological replicates and Mean (CSA: n = 3, N = 1 at 4 wks and n = 3, N = 2 at 8 wks). Two-tailed student t-test. *$P<0.05$, ns = not significant.
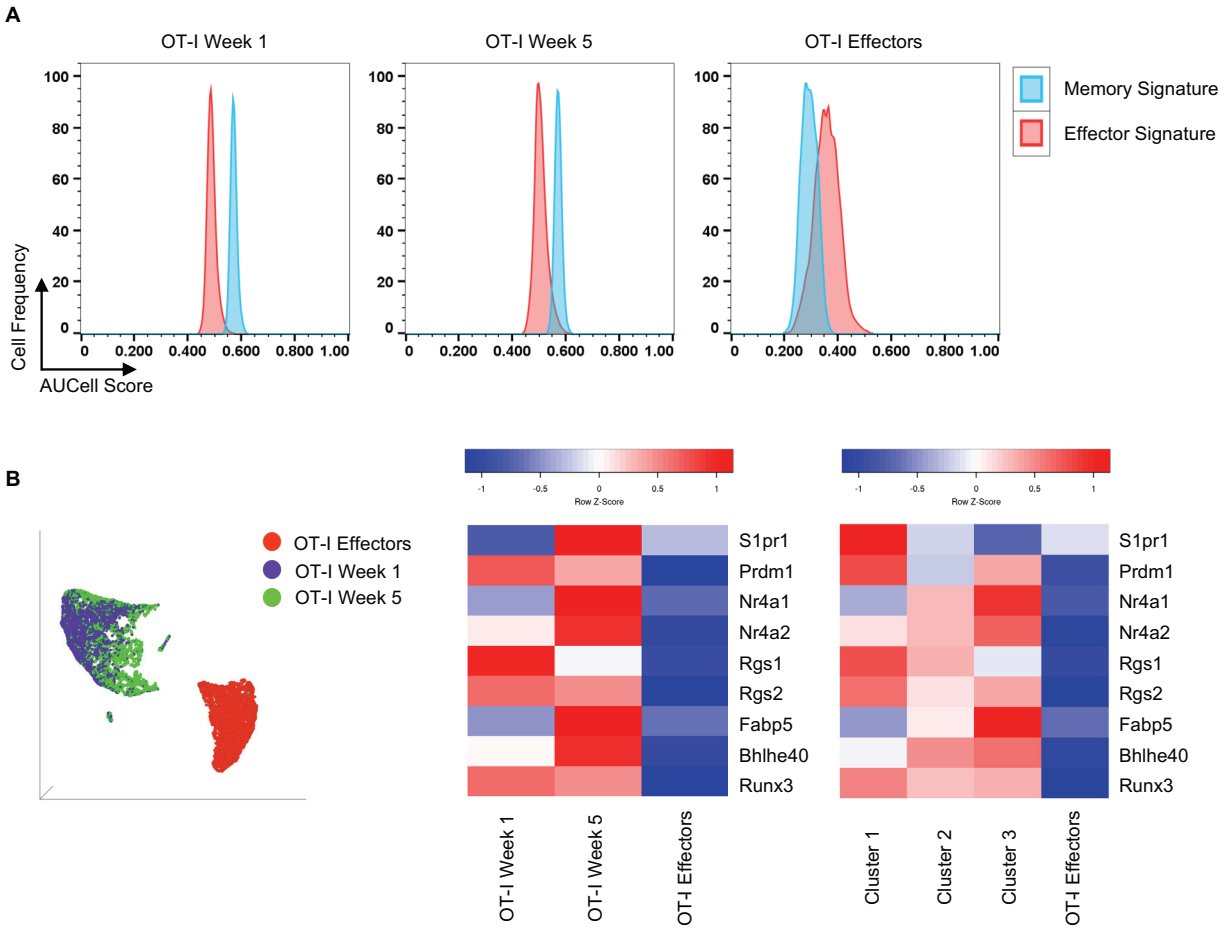
Figure S2. Transcriptomic comparison among OT-I populations. A, AUCell scores of graft OT-I cells at both week 1 and week 5 timepoints and of published circulating OT-I effector cells. **B**, Batched analysis of the published circulating OT-I effector scRNAseq dataset combined with graft OT-I dataset. UMAP shown on the left and heatmaps of T_{RM} gene signature shown on the right.
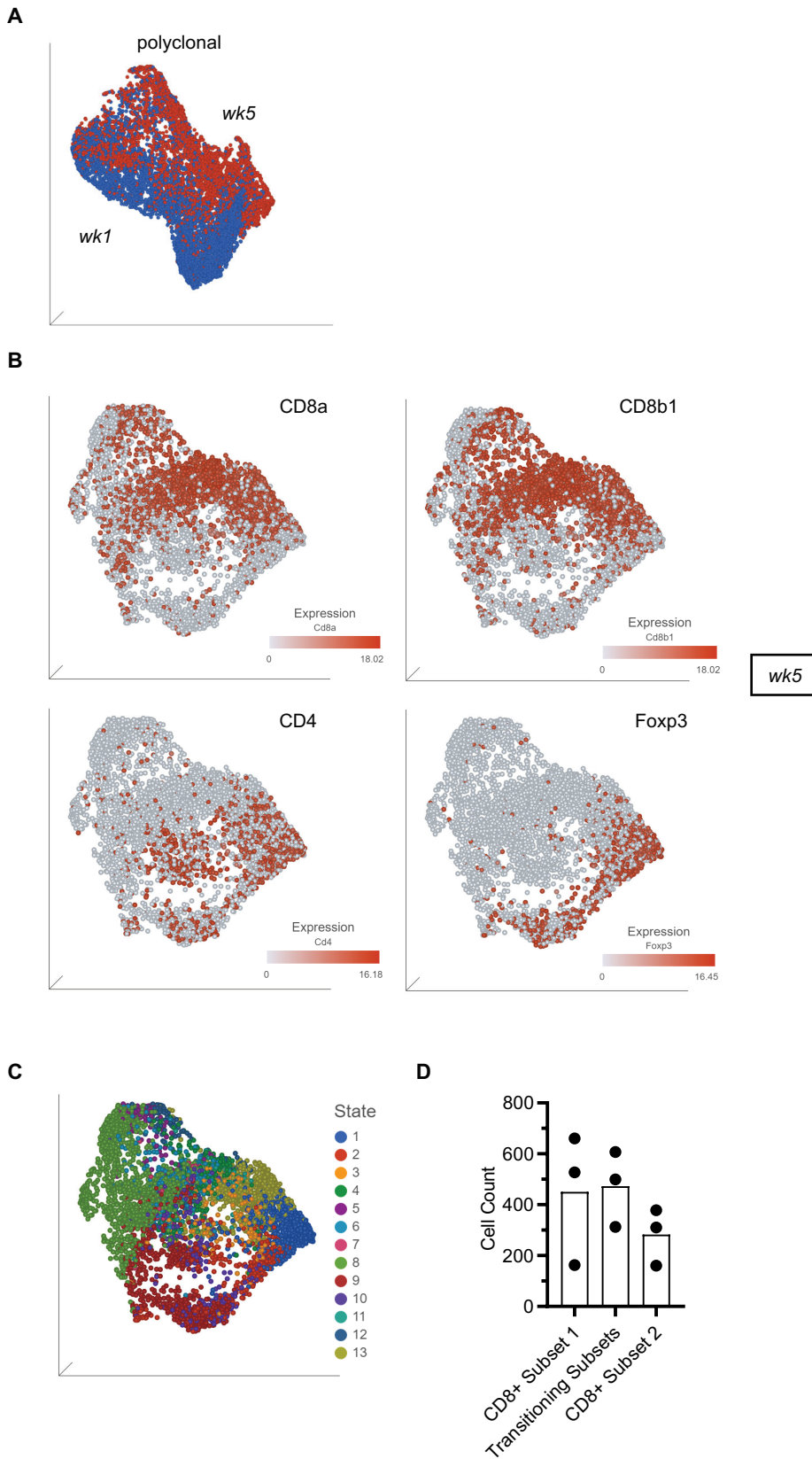
Figure S3. Single cell RNA sequencing analysis of graft polyclonal T cells – classification strategy. **A,** Uniform Manifold Approximation and Projection (UMAP) of combined week 1 and week 5 polyclonal T cells, with cells from either timepoint labeled as shown. **B,** Expression of CD8a, CD8b1, CD4, and Foxp3 genes in UMAP of week 5 polyclonal T cells. **C,** Pseudotime states highlighted in UMAP of week 5 polyclonal T cells. **D**, Quantification of CD8+ subsets shown in Fig. 3E.
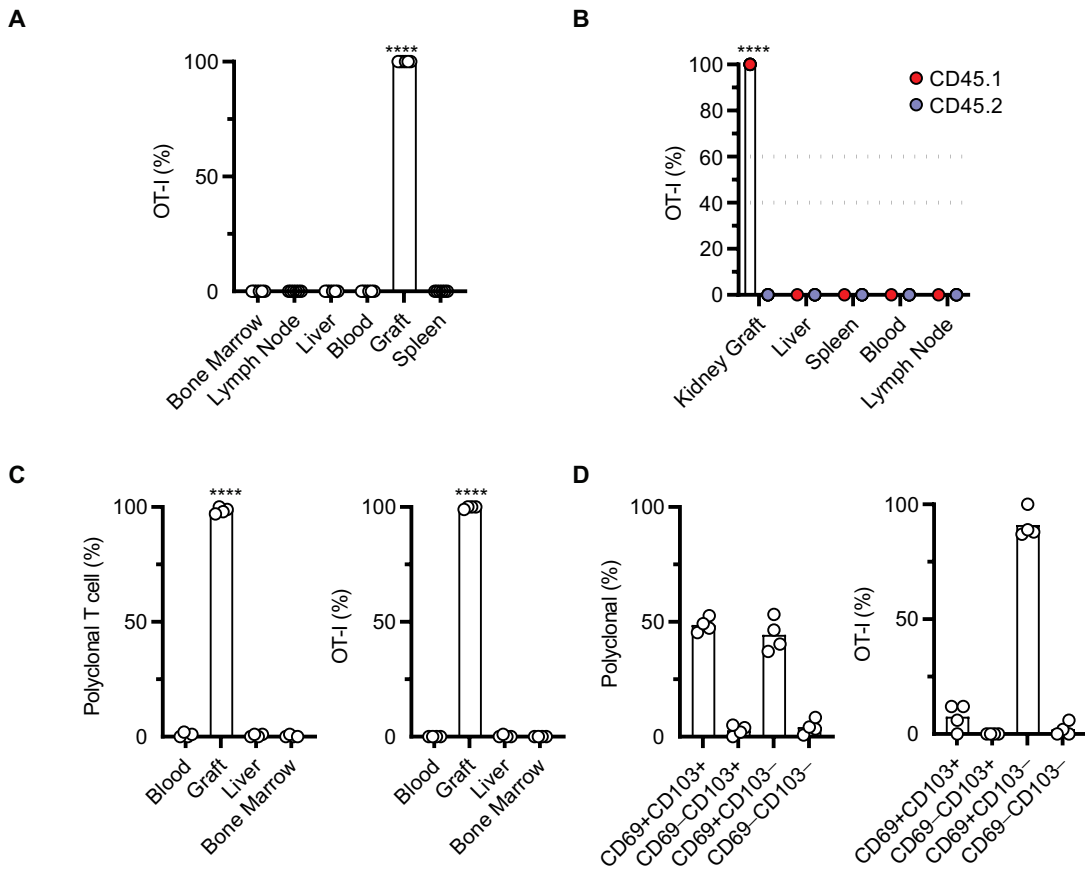
Figure. S4. Quantitation of flow data from Fig. 4. Bar graph representation of flow cytometry data shown in Figs. 4A, C, F, and G, respectively. One-way analysis of variance (ANOVA) (A, B, and C). ****$P<0.0001$
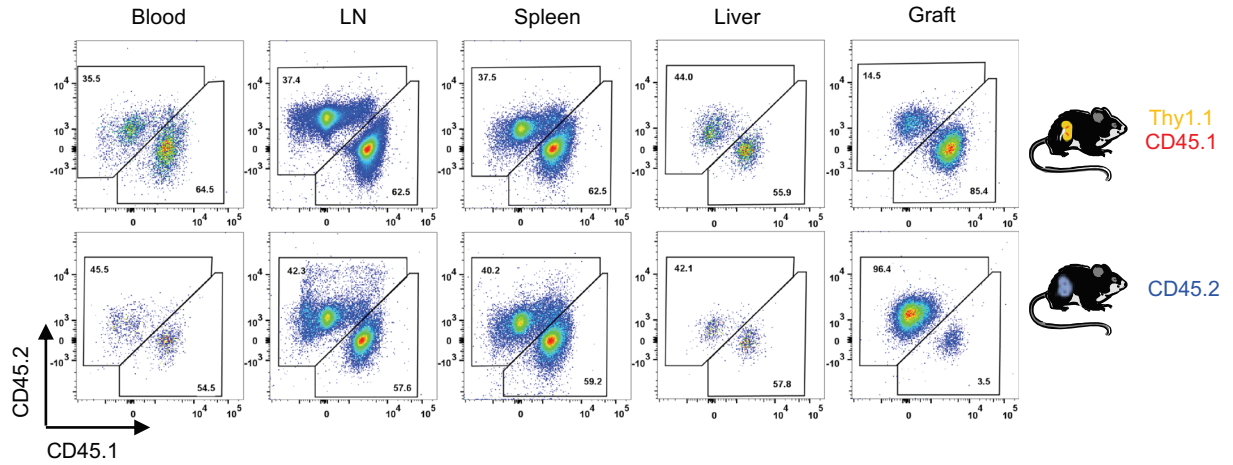
Gated on extravascular CD8+ (except for blood)

Figure S5. Distribution of polyclonal CD8+ T cells in tissues and allografts of parabionts.
Polyclonal CD8+ T cells from either host equilibrated in the livers, spleens, blood, and lymph nodes of both parabionts (parabiosis model is shown in Fig. 4B), demonstrating that the parabiosis was successful, but did not equilibrate in either graft. Representative of 4 parabiosis pairs.
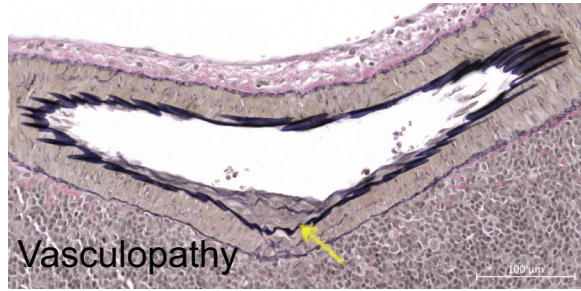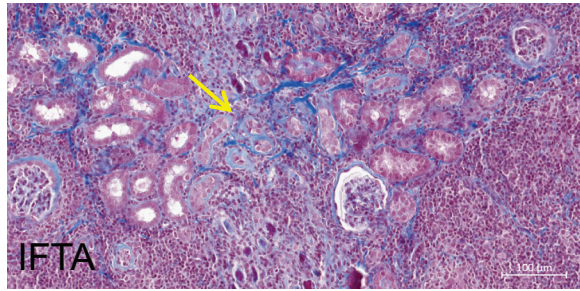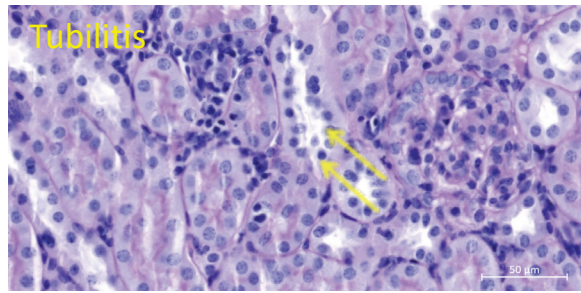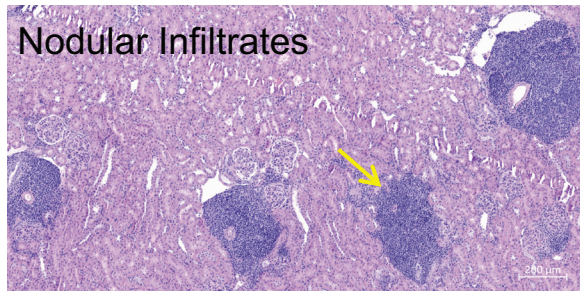
Figure. S6. **Representative pathology in retransplanted kidneys** (n = 4) consistent with chronic active T cell mediated rejection and chronic rejection. IFTA = Interstitial Fibrosis and Tubular Atrophy
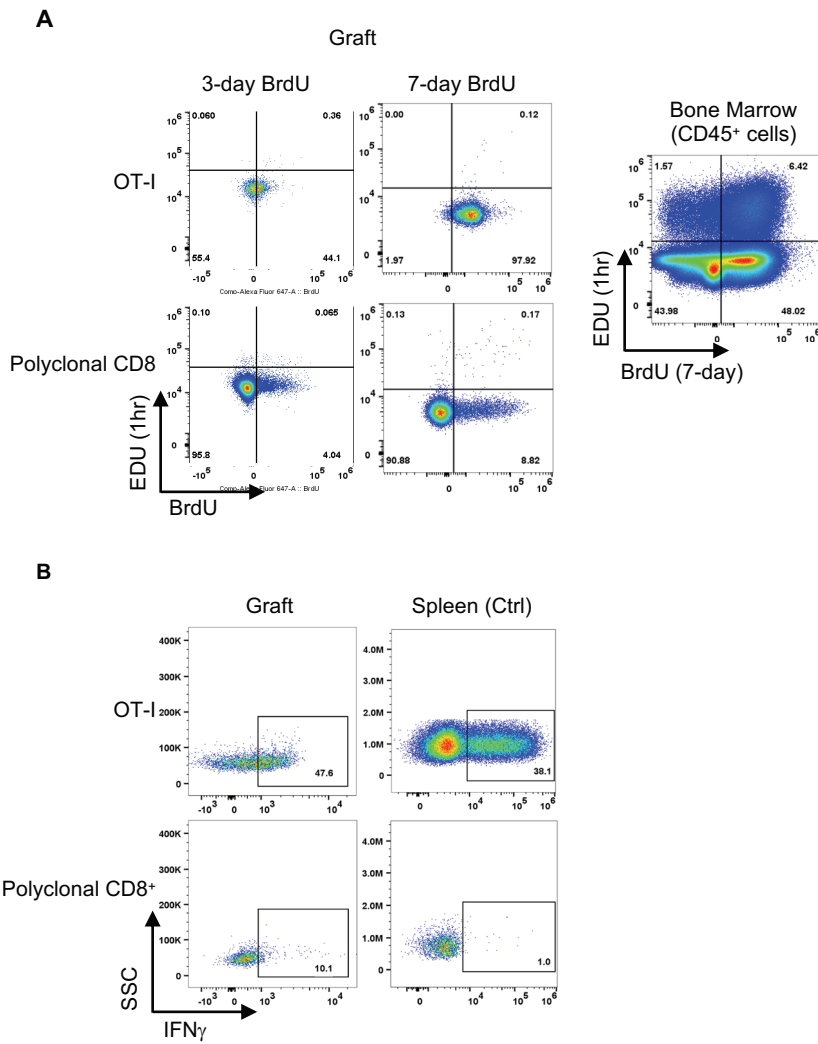
A

Graft

B

Figure S7. Proliferation and IFNγ production in graft OT-I and polyclonal CD8$^+$ T$_{RM}$. A, Representative flow panels depicting Edu and BrdU uptake of week 8 OT-I and polyclonal CD8$^+$ graft T cells after gating on the extravascular CD8$^+$CD44^{hi}CD62L^{lo}CD69$^+$CD103$^{+/-}$ population. Edu was injected i.p. 1 hr prior to harvest. BrdU was administered p.o. for 3 or 7 days prior to harvest. Bone marrow plot shown as positive control. Representative of 4 biological replicates for day 3 and 2 for day 7. **B,** Representative flow panels showing intracellular IFNγ staining post ex vivo allostimulation of graft lymphocytes after gating on OT-I and polyclonal CD8$^+$ T cells (n = 5). Spleen (Ctrl) plot represents IFNγ production by splenocytes from untransplanted mice harboring effector OT-I cells (n = 3, N = 1).
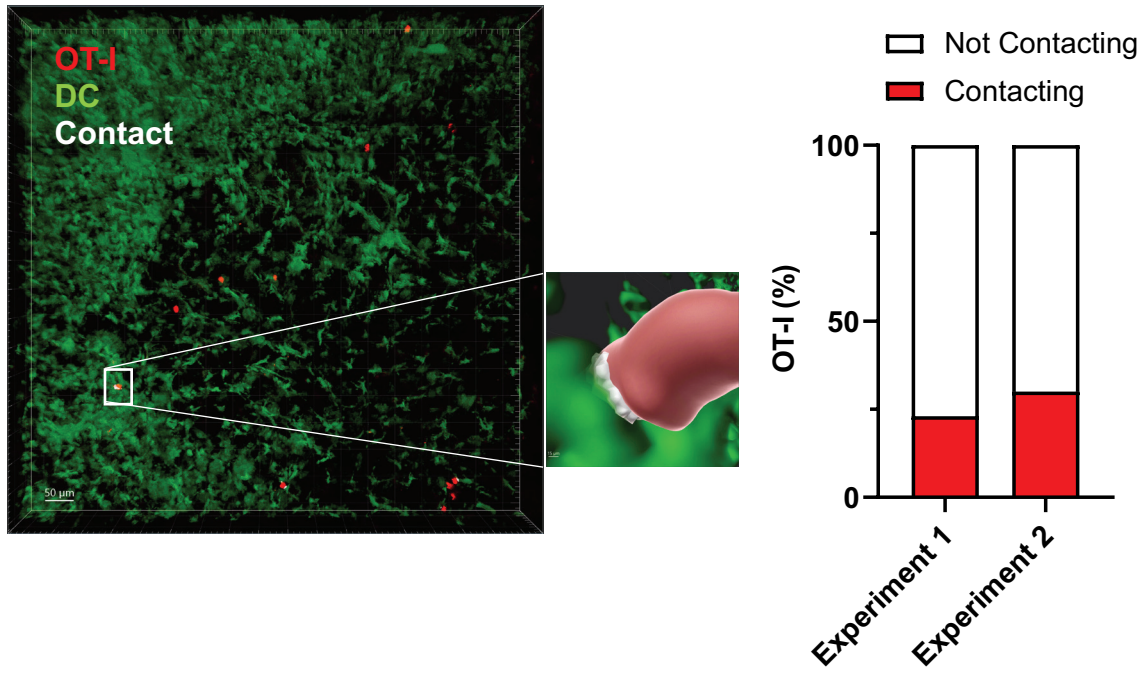
Figure S8. Intravital two-photon microscopy of F1.OVA kidney graft 6 weeks after transplantation into B6.CD11c-YFP recipient adoptively transferred with 1 million effector OT-I.Rag$^{-/-}$Dsred T cells 2 days after transplantation. Image shows DC (green), OT-I (red), and contact areas (white). Enlarged image shows representative contact between OT-I and DC. Graph represents proportion of OT-I cells contacting DCs for >2 min in a 30 min imaging window. n = 2, N = 1.
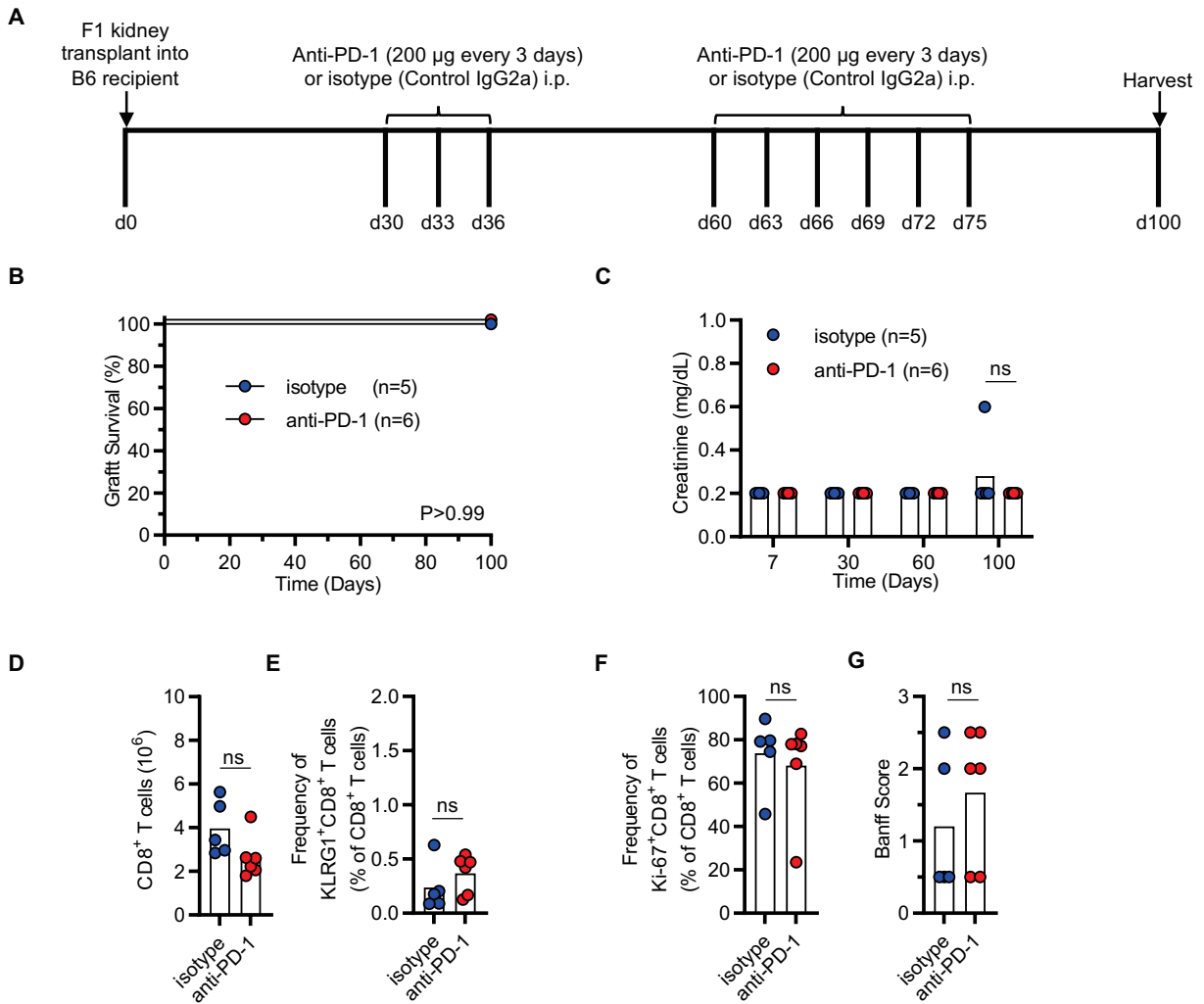
Figure S9. Anti-PD-1 treatment does not enhance rejection. A, Timing of treatment with anti-PD-1 (n = 6, N = 1) or IgG2a isotype control (n = 5, N = 1) antibody in B6 recipients of (Balb/c x B6)F1 kidney allografts. **B-C,** Allograft survival (B) and serum creatinine measurement (C) in isotype and anti-PD-1 treated recipients. **D-G,** Quantification of total graft $CD8^+$ T cells (D), proportion of $CD8^+$ T cells that are $KLRG1^+$ (E) or $Ki-67^+$ (F), and pathology scores (G) in both groups. Data shown are individual biological replicates and Mean. Two-tailed student t-test (B, C, D, E, F and G), and log-rank test (C), ns = not significant.
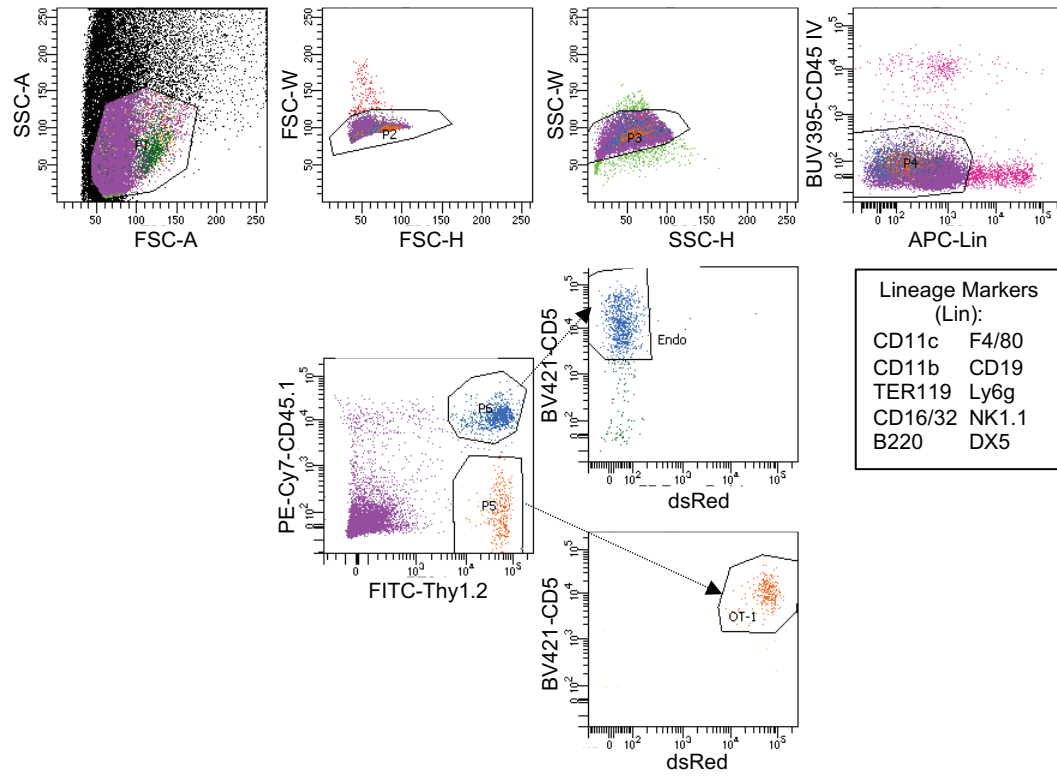
Figure S10. Flow cytometry sorting strategy of graft OT-I and polyclonal T cells for scRNAseq.
Thy1.2 staining and dsRed were used to identify the OT-I cells, and CD45.1 and CD5 staining to
identify polyclonal T cells (Endo), after excluding intravascular cells and lineage markers shown in box.